High-resolution FTIR measurement of the ν 4 band of methylene fluoride-d 2

ARTICLE *in* JOURNAL OF MOLECULAR SPECTROSCOPY · OCTOBER 2004

Impact Factor: 1.48 · DOI: 10.1016/j.jms.2004.06.008

3 AUTHORS, INCLUDING:

Aparna Shastri

Bhabha Atomic Research Centre

32 PUBLICATIONS **74** CITATIONS

SEE PROFILE

Available online at www.sciencedirect.com
SCIENCE DIRECT®
Journal of Molecular Spectroscopy 227 (2004) 195–201
Journal of MOLECULAR SPECTROSCOPY
www.elsevier.com/locate/jms

High-resolution FTIR measurement of the v_4 band of methylene fluoride-d_2

Aparna Shastri,[a] M.N. Deo,[b,*] and K. Kawaguchi[c]

[a] *Spectroscopy Division, Bhabha Atomic Research Centre, Trombay, Mumbai 400 085, India*
[b] *Synchrotron Radiation Section, Bhabha Atomic Research Centre, Trombay, Mumbai 400 085, India*
[c] *Department of Chemistry, Faculty of Science, Okayama University, Tsushima-naka 3-1-1, Okayama 700-8530, Japan*

Received 29 April 2004
Available online 10 July 2004

Abstract

A high-resolution ($0.002\,cm^{-1}$) infrared absorption spectrum of methylene fluoride-d_2 (CD_2F_2) of the lowest fundamental mode v_4 in the region from 460 to $610\,cm^{-1}$ has been measured on a Bruker IFS 120-HR Fourier transform infrared spectrometer. More than 3500 transitions have been assigned in this *B*-type band centered at $521.9\,cm^{-1}$. The data have been combined with upper state pure rotational measurements in a weighted least-squares fit to obtain molecular constants for the upper state resulting in an overall standard deviation of $0.00018\,cm^{-1}$. Accurate value for the band origin ($521.9578036\,cm^{-1}$) has been obtained and inclusion of transitions with very high J ($\leqslant 60$) and K_a ($\leqslant 34$) values has resulted in improved precision for sextic centrifugal distortion constants, in particular D_K, H_{KJ}, and H_K.

Keywords: FTIR; v_4 band; CD_2F_2; *B*-type band

1. Introduction

There has been obvious interest in the high-resolution infrared spectrum of CH_2F_2 and its isotopomer in particular CD_2F_2 [1–7] due to their importance as an efficient laser medium for generation of far-IR laser emission [1,8–10] optically pumped by CO_2 lasers. Prior studies of the spectrum of CD_2F_2 include the first report of the microwave spectrum by Hirota et al. [11]. Subsequently Hirota and Sahara [12] reinvestigated the microwave spectrum in greater detail up to $J = 19$ and determined rotational constants and quartic centrifugal distortion constants of the ground state and a few excited vibrational states. The millimeter/sub-millimeter wave spectra of the ground state and the v_4 ($v = 1$) state has been studied by Deo and Kawaguchi [5] who obtained higher order centrifugal distortion constants by including higher J and K_a transitions.

CD_2F_2 is a near-prolate asymmetric top ($\kappa = -0.89$) and the vibrational assignments ($4a_1 + a_2 + 2b_1 + 2b_2$) of the nine fundamental modes under C_{2V} point group has been reasonably well established from a normal coordinate analysis [13]. The only IR inactive a_2 mode (v_5) does show up as a weak feature in the spectrum and its appearance has been attributed to a possible Coriolis interaction with the neighboring fundamental v_7 level. CD stretching fundamentals (v_1, v_6) appear in the $2200\,cm^{-1}$ region and its high-resolution study was reported recently [14]. Analysis of the 9–10 μm region has been limited to the work by Goh et al. [6,7].

In the 9–10 μm region, CD_2F_2 has a very crowded and complex spectrum due to the fact that four (v_3, v_5, v_7 and v_9) out of its nine fundamental modes lie in this region. Analysis of the spectrum in this region is complicated due to strong Coriolis interactions among the various vibrational modes as pointed out by Hirota and Sahara [12] in their microwave study and Goh et al. [6,7] in FTIR studies. In addition to the four fundamental modes there is the possibility of complications from the $2v_4$ level and hot band transitions such as $v_9 + v_4 - v_4$,

* Corresponding author. Fax: +91-22-2550-5151.
E-mail address: mndeo@vsnl.com (M.N. Deo).

0022-2852/$ - see front matter © 2004 Elsevier Inc. All rights reserved.
doi:10.1016/j.jms.2004.06.008

$v_3 + v_4 - v_4$, etc. This is to be expected because the v_4 ($v = 1$) state is low-lying ($v_0 \sim 521\,\mathrm{cm}^{-1}$) and has a considerable population of ~7% at room temperature. Thus a comprehensive study of the v_4 band at high-resolution should be helpful in the analysis of the hot bands in the strongly perturbed 9–10 μm region.

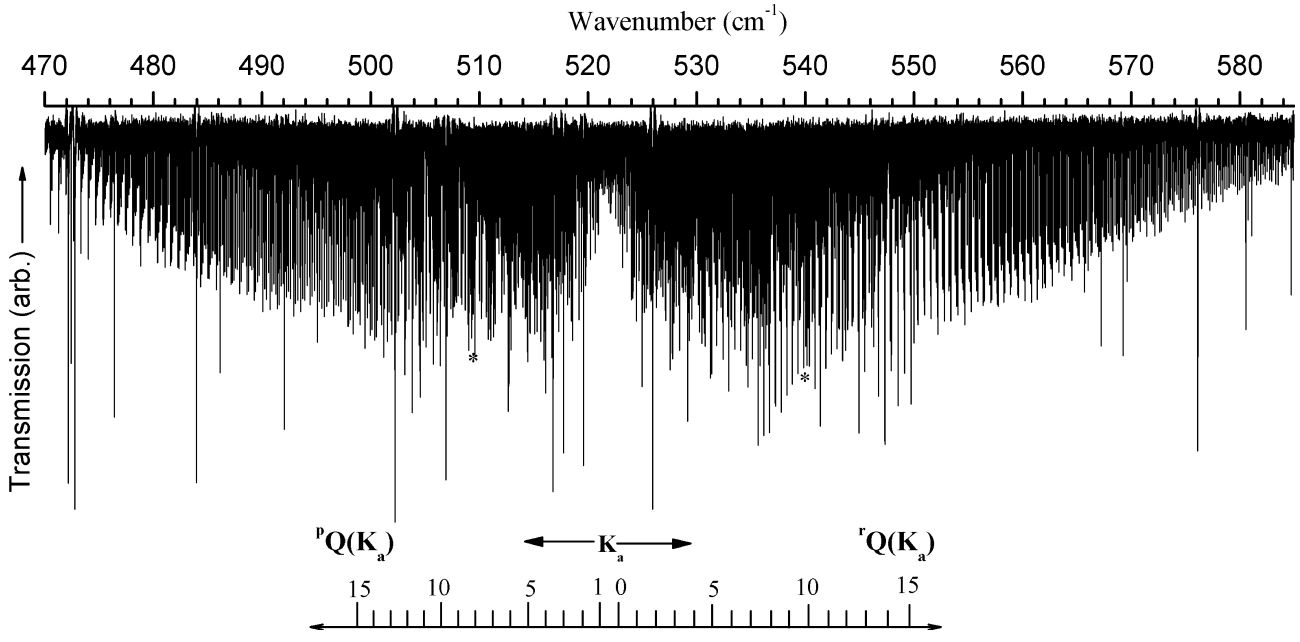

Fig. 1. Overview of the FTIR spectrum of the v_4 Band of CD_2F_2. Pressure = 80 mTorr, path length = 18 m. The asterisks indicate the sub-bands that are shown under high-resolution in Fig. 2.

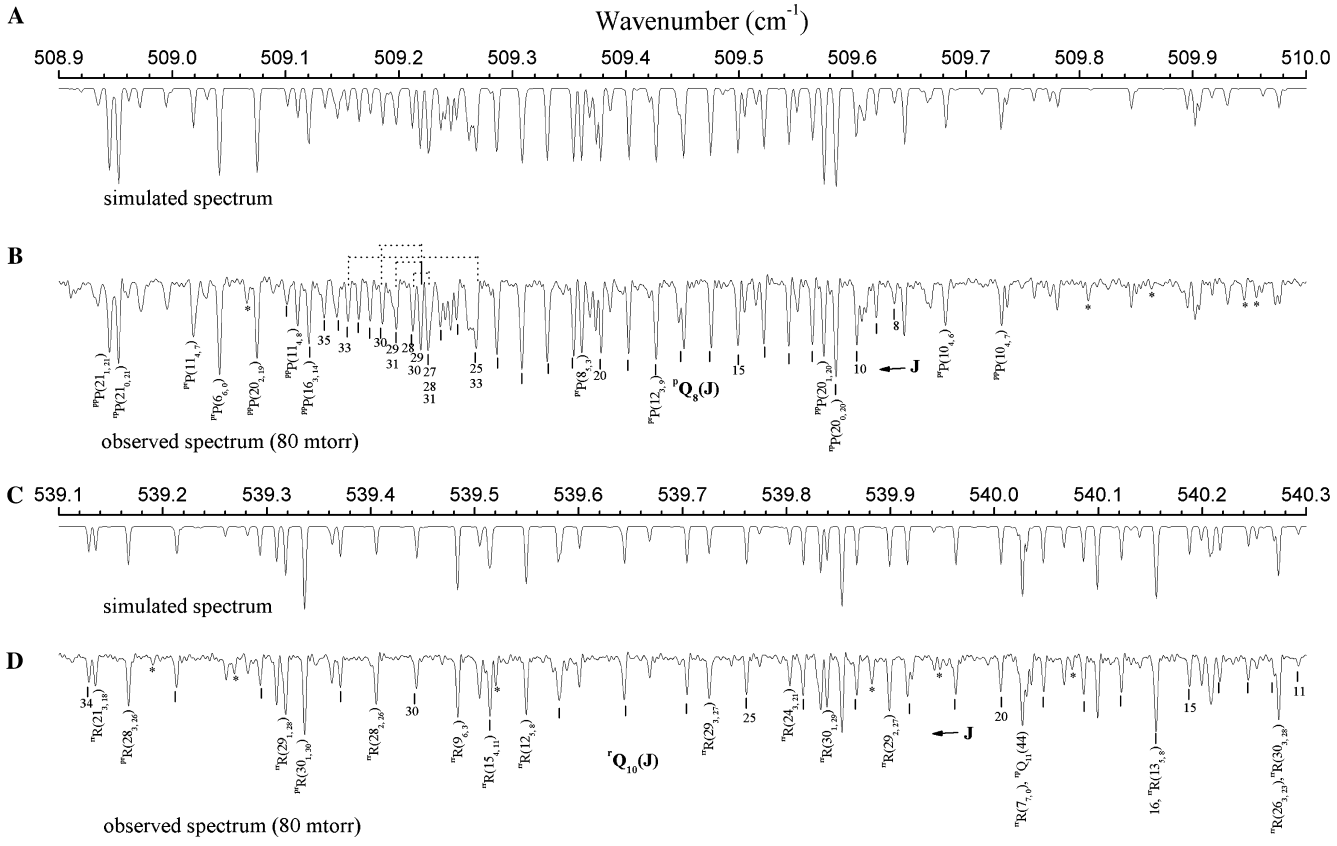

Fig. 2. (A and B) Simulated and observed spectra in the $^pQ_8$-branch region and (C and D) simulated and observed spectra in the $^rQ_{10}$-branch region.The asterisks indicate transitions due to hot bands or impurities.

Table 1
Typical ro-vibrational transitions (in cm^{-1}) of the ν_4 band of CD_2F_2 corresponding to the regions shown in Figs. 2 and 3

J'	K'_a	K'_c	J''	K''_a	K''_c	Obs. freq	O − C[a]
41	7	35	41	8	34	508.93437	58*
20	0	20	21	1	21	508.94466	−38*
34	2	33	34	3	32	508.94466	50*
20	1	20	21	0	21	508.95253	−05
34	1	33	34	2	32	508.96070	−49*
42	5	38	42	6	37	508.97229	23
40	7	34	40	8	33	508.99539	86*
39	9	30	40	8	33	508.99910	00*
10	3	8	11	4	7	509.01859	42
5	5	1	6	6	0	509.04161	07*
39	7	33	39	8	32	509.04161	70*
38	7	32	38	8	31	509.07465	−98*
19	1	18	20	2	19	509.07465	22
37	7	31	37	8	30	509.10108	−16
10	3	7	11	4	8	509.11047	28
36	7	30	36	8	29	509.12054	45*
15	2	13	16	3	14	509.12054	−46*
35	7	29	35	8	28	509.13392	−30
34	7	28	34	8	27	509.14506	−36
33	7	27	33	8	26	509.15496	−16
32	7	26	32	8	25	509.16439	−08
31	7	25	31	8	24	509.17444	09
30	7	24	30	8	23	509.18533	−01
31	1	31	31	2	30	509.19030	−06*
31	0	31	31	1	30	509.19751	73*
29	7	23	29	8	22	509.19751	−32*
28	7	22	28	8	21	509.21212	11
29	7	22	29	8	21	509.21906	−13*
30	7	23	30	8	22	509.21906	38*
27	7	21	27	8	20	509.22552	−44*
28	7	21	28	8	20	509.22552	08*
31	7	24	31	8	23	509.22552	14*
27	7	20	27	8	19	509.23632	10
32	7	25	32	8	24	509.24073	−43
26	7	20	26	8	19	509.24545	−17
26	7	19	26	8	18	509.25058	−01
36	3	34	36	4	33	509.26001	01*
20	3	18	21	2	19	509.26116	−92*
25	7	19	25	8	18	509.26416	−71*
33	7	26	33	8	25	509.26797	−31*
25	7	18	25	8	17	509.26797	18*
24	7	17	24	8	16	509.28615	−06*
34	7	27	34	8	26	509.30825	−25*
23	7	16	23	8	15	509.30825	−09*
22	7	15	22	8	14	509.33059	−17
21	7	14	21	8	13	509.35396	−16
7	4	4	8	5	3	509.36107	06
37	6	31	38	5	34	509.36834	−09*
35	7	28	35	8	27	509.36834	32*
19	2	18	20	1	19	509.37337	−05
20	7	13	20	8	12	509.37810	−01
41	5	37	41	6	36	509.38612	−78*
36	2	34	36	3	33	509.38612	55*
19	7	12	19	8	11	509.40238	−06
33	2	32	33	3	31	509.42053	−01
11	2	10	12	3	9	509.42662	67*
18	7	11	18	8	10	509.42662	−28*
36	7	29	36	8	28	509.44664	−72*
33	1	32	33	2	31	509.44664	69*
17	7	10	17	8	9	509.45118	−04
16	7	9	16	8	8	509.47526	02
15	7	8	15	8	7	509.49885	08

Table 1 (*continued*)

J'	K'_a	K'_c	J''	K''_a	K''_c	Obs. freq	O − C[a]
14	2	12	15	3	13	509.50457	−16
42	6	37	42	7	36	509.51460	−06
14	7	7	14	8	6	509.52160	−01
13	7	6	13	8	5	509.54357	−07
37	7	30	37	8	29	509.55141	14
12	7	5	12	8	4	509.56448	−20
19	0	19	20	1	20	509.57459	−09
19	1	19	20	0	20	509.58527	−58*
11	7	4	11	8	3	509.58527	65*
10	7	4	10	8	3	509.60362	30*
39	3	36	39	4	35	509.60808	−46
22	4	19	23	3	20	509.61167	48
9	7	2	9	8	1	509.62070	02
8	7	2	8	8	1	509.63678	18
18	1	17	19	2	18	509.64546	06
30	0	30	30	1	29	509.66867	−30*
9	3	7	10	4	6	509.68180	39
38	7	31	38	8	30	509.68317	00*
9	3	6	10	4	7	509.73132	07
35	3	33	35	4	32	509.73621	−16
41	6	36	41	7	35	509.76032	13
40	5	36	40	6	35	509.78043	02
39	7	32	39	8	31	509.84575	04
32	2	31	32	3	30	509.89527	−14
13	2	11	14	3	12	509.90191	−16
35	2	33	35	3	32	509.90555	05
32	1	31	32	2	30	509.93078	−25
10	1	10	11	2	9	509.96070	−03*
40	6	35	40	7	34	509.97650	19
34	11	24	34	10	25	539.12900	18
22	4	19	21	3	18	539.13516	10
29	2	27	28	3	26	539.16691	−05
33	11	22	33	10	23	539.21322	12
32	4	28	31	5	27	539.26041	06
17	3	14	16	2	15	539.28156	−14
32	11	22	32	10	23	539.29352	−13
30	1	29	29	2	28	539.30943	09
30	2	29	29	1	28	539.31831	03
31	0	31	30	1	30	539.33646	03
23	4	20	22	3	19	539.36264	11
31	11	20	31	10	21	539.37054	02
29	3	27	28	2	26	539.40529	−06
30	11	20	30	10	21	539.44389	02
10	7	4	9	6	3	539.48362	−01
30	3	27	29	4	26	539.50465	−40
16	5	12	15	4	11	539.51456	−65*
29	11	19	29	10	20	539.51456	76*
13	6	7	12	5	8	539.54966	−16
28	11	18	28	10	19	539.58046	02*
24	4	21	23	3	20	539.58266	−14*
16	5	11	15	4	12	539.60071	04
27	11	17	27	10	18	539.64397	10
18	4	14	17	3	15	539.66836	−05
26	11	16	26	10	17	539.70423	02
30	2	28	29	3	27	539.72550	05
25	11	14	25	10	15	539.76158	02
25	4	22	24	3	21	539.80303	−18
24	11	14	24	10	15	539.81599	00
31	1	30	30	2	29	539.83286	02
31	2	30	30	1	29	539.83890	−07
32	0	32	31	1	31	539.85325	01*
32	1	32	31	0	31	539.85325	−07*
23	11	13	23	10	14	539.86760	00

Table 1 (*continued*)

J'	K'_a	K'_c	J''	K''_a	K''_c	Obs. freq	O − C[a]
30	3	28	29	2	27	539.89886	04
22	11	12	22	10	13	539.91641	−05
36	5	31	35	6	30	539.94187	−04
21	11	10	21	10	11	539.96266	00
20	11	9	20	10	10	540.00633	07
44	12	33	44	11	34	540.02223	−55*
8	8	1	7	7	0	540.02699	−02
26	4	23	25	3	22	540.03131	07
44	7	37	43	8	36	540.03519	−26
19	11	8	19	10	9	540.04726	−09
17	5	13	16	4	12	540.06729	18
58	2	56	58	1	57	540.07447	−44
18	11	8	18	10	9	540.08589	−07
11	7	4	10	6	5	540.09922	−07
17	11	7	17	10	8	540.12223	03
40	6	34	39	7	33	540.13231	32
43	12	31	43	11	32	540.13940	−19*
14	6	9	13	5	8	540.15544	57*
16	11	6	16	10	7	540.15544	−65*
15	11	5	15	10	6	540.18771	01
33	4	29	32	5	28	540.19931	−05
17	5	12	16	4	13	540.20754	17
31	3	28	30	4	27	540.20983	03
14	11	4	14	10	5	540.21699	−10
13	11	3	13	10	4	540.24437	09
42	12	31	42	11	32	540.25260	08
12	11	1	12	10	2	540.26911	−25
27	4	24	26	3	23	540.27356	−51*
31	2	29	30	3	28	540.27356	17*
11	11	1	11	10	2	540.29222	−12
34	22	13	34	21	14	560.03900	03
23	14	10	22	13	9	560.07156	−01
36	10	27	35	9	26	560.08723	19
33	22	11	33	21	12	560.10237	15
20	15	6	19	14	5	560.15125	−01
40	9	32	39	8	31	560.16245	42*
17	16	1	16	15	2	560.22228	10*
31	22	9	31	21	10	560.22228	−56*
33	11	22	32	10	23	560.29902	06
29	22	8	29	21	9	560.33549	−21
30	12	19	29	11	18	560.44727	−05
26	22	5	26	21	6	560.49077	22
25	22	4	25	21	5	560.53837	02
27	13	15	26	12	14	560.56394	−06
24	22	3	24	21	4	560.58442	16
41	9	33	40	8	32	560.62343	34*
37	10	28	36	9	27	560.62665	17
37	10	27	36	9	28	560.62940	−15
24	14	11	23	13	10	560.66227	−09
50	23	28	50	22	29	560.71035	−21
21	15	7	20	14	6	560.74870	07
18	16	3	17	15	2	560.82570	03
34	11	24	33	10	23	560.85831	00
31	12	19	30	11	20	561.01916	02
42	9	34	41	8	33	561.06206	−10
28	13	16	27	12	15	561.14497	−07
38	10	29	37	9	28	561.16074	06
38	10	28	37	9	29	561.16564	01
25	14	12	24	13	11	561.25095	−04
40	6	34	39	5	35	561.30965	07
43	23	20	43	22	21	561.33118	−39
22	15	7	21	14	8	561.34402	07
42	9	33	41	8	34	561.35305	09

Table 1 (*continued*)

J'	K'_a	K'_c	J''	K''_a	K''_c	Obs. freq	O − C[a]
44	8	36	43	7	37	561.40336	17
35	11	24	34	10	25	561.41430	04
19	16	4	18	15	3	561.42724	04
43	9	35	42	8	34	561.47482	21
32	12	21	31	11	20	561.58817	02
39	23	17	39	22	18	561.64193	−03
39	10	30	38	9	29	561.68928	07
39	10	29	38	9	30	561.69714	07
29	13	17	28	12	16	561.72356	−10
31	2	29	30	1	30	561.78528	−17*
37	23	15	37	22	16	561.78528	02*
43	7	36	42	6	37	561.79158	−05
26	14	13	25	13	12	561.83752	11
44	9	36	43	8	35	561.85490	−25
43	9	34	42	8	35	561.88415	06
23	15	9	22	14	8	561.93715	−05
36	11	26	35	10	25	561.96648	−01
49	22	28	48	21	27	590.01847	17*
28	28	1	27	27	0	590.02625	10
35	26	9	34	25	10	590.10016	14*
42	24	19	41	23	18	590.10016	−11*
53	21	33	52	20	32	590.20433	−33
46	23	23	45	22	24	590.34394	08
57	20	37	56	19	38	590.34920	−30
32	27	6	31	26	5	590.36051	09
39	25	15	38	24	14	590.39095	05
50	22	29	49	21	28	590.55578	10*
29	28	2	28	27	1	590.60968	02
43	24	20	42	23	19	590.65432	−10
36	26	10	35	25	11	590.66936	19
54	21	34	53	20	33	590.73136	−24
47	23	25	46	22	24	590.88872	04
33	27	6	32	26	7	590.93592	09
40	25	16	39	24	15	590.95157	01
51	22	30	50	21	29	591.09072	−03
30	28	3	29	27	2	591.19127	07
44	24	20	43	23	21	591.20631	05
37	26	12	36	25	11	591.23629	01
55	21	35	54	20	34	591.25622	12
59	20	40	58	19	39	591.37809	50*
48	23	25	47	22	26	591.43116	−11
34	27	8	33	26	7	591.50958	36
41	25	17	40	24	16	591.50958	−50*
52	22	31	51	21	30	591.62344	−05
45	24	21	44	23	22	591.75601	07
31	28	3	30	27	4	591.77079	03
56	21	36	55	20	35	591.77835	22
38	26	13	37	25	12	591.80136	02
60	20	41	59	19	40	591.88814	48*
49	23	27	48	22	26	591.97155	−06
42	25	18	41	24	17	592.06660	03
35	27	8	34	26	9	592.08067	07
53	22	32	52	21	31	592.15405	18
57	21	36	56	20	37	592.29765	−01*
46	24	22	45	23	23	592.30333	−11
32	28	5	31	27	4	592.34842	10
39	26	14	38	25	13	592.36443	11

[a] O − C = (observed − calculated) × 10^5 cm^{-1}.

* The symbol indicates lines not included in the fit.

In the present work, the FTIR spectrum of the ν_4 band has been recorded under high-resolution and analyzed in order to obtain the band origin and other

molecular parameters accurately. Also since transitions with high J ($\leqslant 60$) and K_a ($\leqslant 34$) have been observed the precision of the J and K_a dependent parameters has greatly improved compared to previous reports [5].

2. Experiment

Fourier transform absorption spectra of CD_2F_2 between 470 and 610 cm^{-1} were measured at an apodized spectral resolution of 0.002 cm^{-1} on a Bruker IFS 120HR FTIR spectrometer using a globar infrared source, KBr beamsplitter and an appropriate optical filter. Spectra were recorded with two detectors, liquid helium cooled Ge-bolometer and liquid nitrogen cooled HgCdTe (MCT) for the region 470–550 and 520–610 cm^{-1}, respectively. The spectra were obtained with a multiple pass cell set at a path length of 18 m and at sample pressures of 0.08, 0.20, 0.66, and 1.8 Torr in order to measure low as well as high J and K_a transitions. For each set, about 180 scans were co-added for a total integration time of 12 h. The reference spectra of the empty cell at lower resolution was recorded for a duration of 5 h, which was, after zero fillings, used to reduce water vapour lines and to get good base line. Residual water vapour lines were used for calibration. The accuracy of the measurement is expected to be better than 0.00025 cm^{-1}. The observed overall high-resolution features are shown in Fig. 1, in a condensed scale.

3. Analysis, results, and discussions

CD_2F_2 is a near-prolate asymmetric rotor with $\kappa = -0.89$ and belongs to the C_{2V} point group. The ν_4 mode ascribes to the CF_2 scissoring motion [13] which produces a dipole moment change parallel to the intermediate axis of moment of inertia, thus giving rise to a B-type band. The strong transitions are determined by the selection rules

$$\Delta K_a = \pm 1, \quad \Delta K_c = \pm 1, \quad \text{with } \Delta J = 0, \pm 1$$

for a B-type band the allowed transitions are of the type ee $\leftrightarrow$ oo and eo $\leftrightarrow$ oe.

Transitions originating from oe or eo levels have a nuclear spin statistical weight of 21 compared to 15 for transitions from other levels. Transitions from corresponding levels therefore show an intensity alternation with a ratio 21:15. This feature is useful in checking line assignments. The ν_4 mode being the lowest vibrational state above the ground state is well isolated from other vibrational levels, hence it is free from perturbations. However, the observed band may be complicated due to the presence of overlapping hot bands and the presence of impurities such as $CHDF_2$ (~0.5%) and $^{13}CD_2F_2$ (natural abundance ~1%).

Since CD_2F_2 is a near-prolate asymmetric top with an asymmetric parameter, $\kappa = -0.89$, the B-type band is expected to bear a close resemblance to the perpendicular band of a symmetric top molecule. Spectra are

Table 2A
Molecular parameters (in cm^{-1}) for the ν_4 ($v = 1$) band of CD_2F_2[a] S-reduction; I^r representation

Parameter	Ground state[b]	ν_4 ($v = 1$) state	
		Present	Previous[b]
ν_0	–	521.9578036(39)	–
A	1.15897681(1)	1.16501523(1)	1.16501530(3)
B	0.341618053(5)	0.340867516(5)	0.340867505(8)
C	0.294597299(5)	0.293470927(5)	0.293470917(8)
$D_J \times 10^6$	0.3111105(52)	0.3076311(57)	0.307607(15)
$D_{JK} \times 10^6$	−0.986060(22)	−0.971075(23)	−0.971171(54)
$D_K \times 10^5$	0.7809106(55)	0.8000726(97)	0.80029(10)
$\delta_J \times 10^7$	−0.667962(11)	−0.664413(14)	−0.664413(20)
$\delta_K \times 10^8$	−0.380616(37)	−0.404174(50)	−0.404108(74)
$H_J \times 10^{12}$	0.3329(17)	0.3189(19)	0.3069(69)
$H_{JK} \times 10^{12}$	0.3209(87)	0.371(12)	0.373(20)
$H_{KJ} \times 10^{10}$	−0.46809(85)	−0.47843(48)	−0.4905(60)
$H_K \times 10^9$	0.18331(14)	0.191236(84)	0.209(11)
$h_J \times 10^{12}$	0.17696(48)	0.17100(65)	0.17108(98)
$h_{JK} \times 10^{13}$	0.2878(30)	0.3067(40)	0.3045(61)
$h_K \times 10^{14}$	0.3856(61)	0.4232(93)	0.415(13)
Standard deviation		0.000176 cm^{-1}	

[a] Standard deviations given in parentheses are 1σ in terms of the last digit quoted.
[b] Values taken from [5].

Table 2B
Molecular parameters (in cm^{-1}) for the ν_4 ($v = 1$) band of CD_2F_2[a] A-reduction; I^r representation

Parameter	Ground state[b]	ν_4 ($v = 1$) state	
		Present	Previous[b]
ν_0	—	521.9578036(39)	—
A	1.15897676(1)	1.16501519(1)	1.16501525(3)
B	0.341619157(5)	0.340868687(5)	0.340868678(8)
C	0.294596222(5)	0.293469784(5)	0.293469775(8)
$\Delta_J \times 10^6$	0.3187199(53)	0.3157099(58)	0.315687(15)
$\Delta_{JK} \times 10^5$	−0.1031775(23)	−0.1019614(23)	−0.1019692(53)
$\Delta_K \times 10^5$	0.7847184(55)	0.8041177(96)	0.80433(10)
$d_J \times 10^7$	0.667974(10)	0.664416(13)	0.664421(19)
$d_K \times 10^6$	0.544954(50)	0.578834(66)	0.57871(10)
$\Phi_J \times 10^{12}$	0.3895(18)	0.3783(20)	0.3668(71)
$\Phi_{JK} \times 10^{11}$	0.2185(41)	0.2401(57)	0.2386(81)
$\Phi_{KJ} \times 10^{10}$	−0.5406(14)	−0.5571(19)	−0.5687(60)
$\Phi_K \times 10^9$	0.18869(16)	0.19707(15)	0.215(10)
$\varphi_J \times 10^{12}$	0.18107(52)	0.17505(68)	0.1754(10)
$\varphi_{JK} \times 10^{12}$	0.411(44)	0.498(59)	0.439(89)
$\varphi_K \times 10^{10}$	0.5161(86)	0.555(13)	0.547(18)
Standard deviation		0.000176 cm^{-1}	

[a] Standard deviations given in parentheses are 1σ in terms of the last digit quoted.
[b] Values taken from [5].

therefore characterized by prominent Q branches with a separation of $\sim 2(A-\bar{B})$ where $\bar{B}=(B+C)/2$. In this case, $2(A-\bar{B})$ is about $1.7\,\mathrm{cm}^{-1}$. Since for CD_2F_2 $A>\bar{B}$, the separation of successive Q branches $2(A-\bar{B})$ is much greater than the separation of the P and R lines in each sub-band given by $\sim 2\bar{B}$ ($\sim 0.6\,\mathrm{cm}^{-1}$). Thus it is seen that Q branches for different K_a values spread out (Fig. 1) whereas within a K_a sub-band lines with different J cluster together. Two such Q branches, one in the P-branch and another in the R-branch region are shown in Fig. 2. Since the rotational constants for the ground as well as for the v_4 state were available from recent pure rotational spectra in the millimeter and sub-millimeter wave [5] region, spectra were simulated in the region of the predicted band center near $521.7\,\mathrm{cm}^{-1}$ from low-resolution studies [13]. The value of the band origin was then adjusted until the simulated spectra resembled the characteristic Q-branch features in the observed spectra. The assignment of Q-branch features with low K_a values was complicated due to large asymmetry splittings. Sub-bands with $K_a>5$ give rise to characteristic features free from asymmetry splittings for moderate J values and could be more readily identified. Assignment of transitions was done via a bootstrap procedure, initially using the method of combination differences and later by predicted line positions from the refined molecular constants. Data were analyzed with a least-squares fit program using Watsons' A-reduced Hamiltonian [15] in the I^r representation. The assignments were gradually extended to include higher J and K_a transitions. In this manner a total of about 3500 ro-vibrational transitions have been assigned. In the final fitting, about 3100 FTIR data were combined with microwave [12] and millimeter wave [5] data of the upper state with appropriate weighting factors. Lines with deviation $>0.0007\,\mathrm{cm}^{-1}$ were excluded from the fit and lines not split by asymmetry were included only once. Standard deviations of the independent fits of various data sets (σ_i) were used as weights ($1/\sigma_i^2$) in the combined weighted least-squares analysis. The overall standard deviation of the FTIR

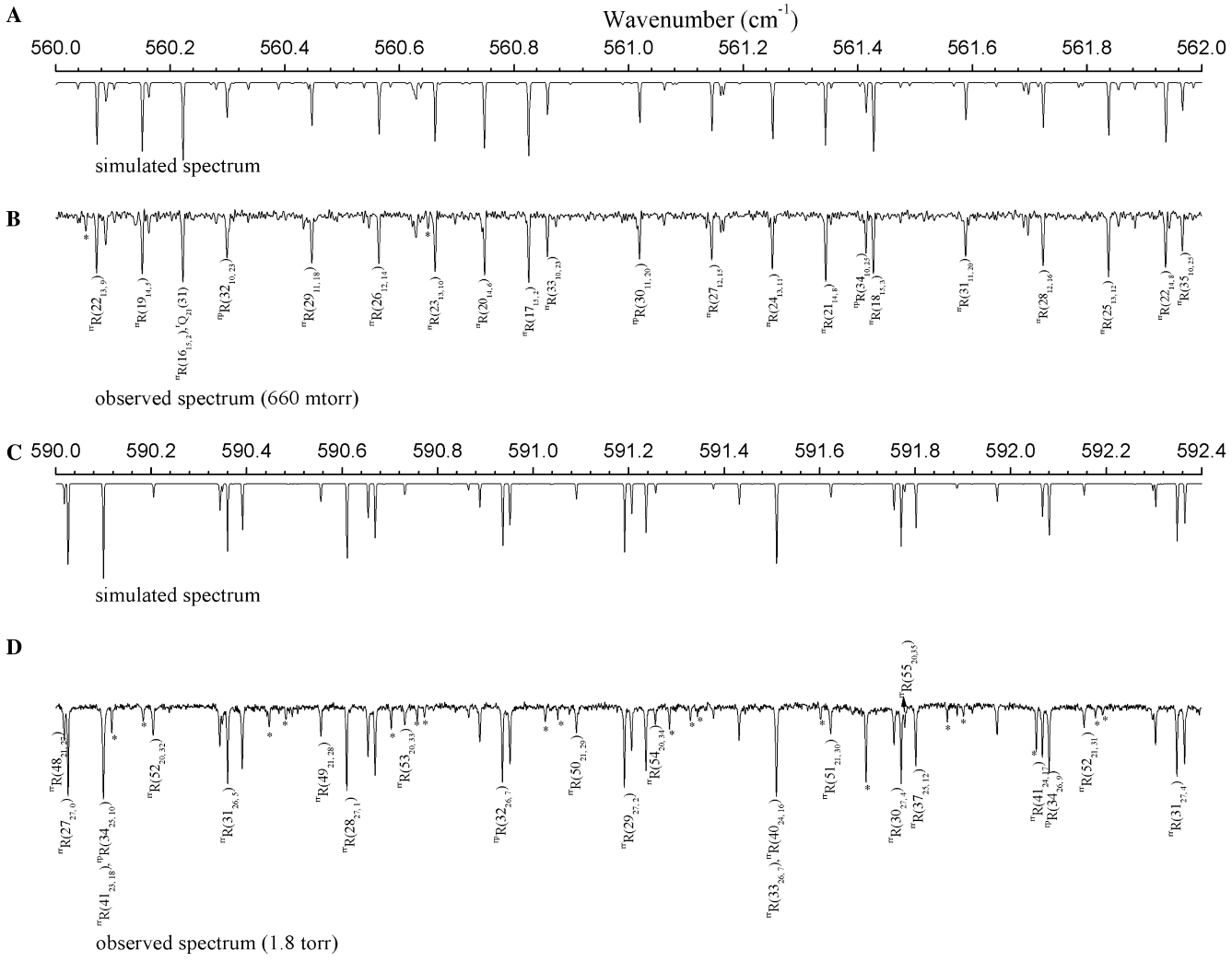

Fig. 3. (A and B) Simulated and observed spectra in the R-branch region, medium J, K_a. (C and D) Simulated and observed spectra in the R-branch region, high J, K_a. The asterisks indicate transitions due to hot bands or impurities.

data was found to be $0.00018\,cm^{-1}$ which is well within the experimental uncertainty. Since the FTIR data set is very large only a few ro-vibrational transitions have been listed in Table 1 as a representative of the quality of the fit. Complete set of data can be obtained on request from the authors.

The S-reduction in the I^r representation is the obvious choice for CD_2F_2 ($\kappa = -0.89$) but for comparison with previous reported results we have carried out the calculation in the S-reduction as well as in the A-reduction. The molecular parameters obtained are listed in Tables 2A and 2B along with previously reported values for comparison. It can be seen that the precision of parameters in particular D_k, H_{KJ}, H_K, etc. has improved considerably. This is because higher K_a transitions were included in the present study, which helped in improving the K dependent parameters.

As a final confirmation of the assignments computer simulation of the spectra was carried out with the molecular parameters reported in Table 2A. The simulated spectra are compared with the observed spectra in Figs. 2 and 3. Fig. 2 shows the simulated spectra along with the experimentally observed spectra of ${}^pQ_8$ and ${}^rQ_{10}$ in the P- and R-branch region, respectively. Fig. 3 shows R-branch transitions in the region of medium and higher K_a transitions. It can be seen that there is excellent agreement between the observed and simulated spectra with respect to line positions as well as relative intensities of spectral lines. A few extra weak features appearing in the observed spectra could be attributed to either hot band transitions ($2\nu_4 \leftarrow \nu_4$) or due to the presence of $CHDF_2$ ($\sim$0.5%) as impurity and $^{13}CD_2F_2$ which has about 1% natural abundance in the sample. Hot band transition $2\nu_4 \leftarrow \nu_4$ is expected as ν_4 ($v = 1$) state has about 7% population at room temperature.

In conclusion, more than 3500 lines in the high-resolution FTIR absorption spectrum of the ν_4 band of CD_2F_2 were assigned. Out of these 3100 lines were combined with all other available data to obtain a set of very precisely determined molecular parameters for the ν_4 ($v = 1$) state including the band origin. The availability of precise parameters for the ν_4 state may serve as useful input in analyzing the spectrum in the 9–10 μm region where hot band transitions involving ν_4 could occur.

Acknowledgments

Aparna Shastri and M.N. Deo are thankful to Drs. N.C. Das and S.M. Sharma for their interest and encouragement.

References

[1] J.C. Derocoche, E.K. Benichou, G. Guelachvili, J. Demaison, Int. J. Infrared Millim. Waves 7 (1986) 1653–1675.
[2] M.N. Deo, R. D'Cunha, V.A. Job, J. Mol. Spectrosc. 161 (1993) 403–415.
[3] J. Matuszeski, M.D. Marshall, Spectrochim. Acta A 50 (1999) 1069–1077.
[4] K.M. Smith, G. Duxbury, D.A. Newnham, J. Ballard, J. Mol. Spectrosc. 193 (1999) 166–173.
[5] M.N. Deo, K. Kawaguchi, J. Mol. Spectrosc. 196 (1999) 212–219.
[6] K.L. Goh, T.L. Tan, P.P. Ong, H.H. Teo, J. Mol. Spectrosc. 201 (2000) 310–313.
[7] K.L. Goh, T.L. Tan, P.P. Ong, K.H. Chaw, H.H. Teo, Mol. Phys. 98 (2000) 1343–1346.
[8] E.C.C. Vasconcellos, T.R. Peterson, K.M. Evenson, Int. J. Infrared Millim. Waves 2 (1981) 705–711.
[9] J.C. Peterson, D. Igner, G. Duxbury, J. Mol. Spectrosc. 100 (1983) 396–402.
[10] S.C. Zebetto, E.C.C. Vasconcellos, L.R. Zink, K.M. Evenson, Int. J. Infrared Millim. Waves 18 (1997) 2301–2306.
[11] E. Hirota, T. Tanaka, A. Sakakibara, Y. Ohashi, Y. Morino, J. Mol. Spectrosc. 34 (1970) 222.
[12] E. Hirota, M. Sahara, J. Mol. Spectrosc. 56 (1975) 21–38.
[13] I. Suzuki, T. Shimanouchi, J. Mol. Spectrosc. 46 (1973) 130–145.
[14] K.L. Goh, T.L. Tan, P.P. Ong, Chem. Phys. Lett. 323 (2000) 361–364.
[15] J.K.G. Watson, in: J.R. Durig (Ed.), Vibrational Spectra and Structure, vol. 6, Elsevier, Amsterdam, 1977, pp. 1–89.